

pubs.acs.org/synthbio Research Article

A Coculture Based Tyrosine-Tyrosinase Electrochemical Gene Circuit for Connecting Cellular Communication with Electronic Networks

Eric VanArsdale,[§] David Hörnström,[§] Gustav Sjöberg, Ida Järbur, Juliana Pitzer, Gregory F. Payne, Antonius J. A. van Maris, and William E. Bentley*



Cite This: ACS Synth. Biol. 2020, 9, 1117–1128



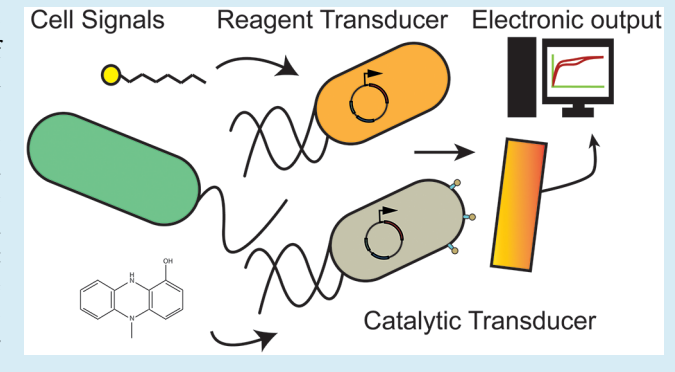
ACCESS

Metrics & More



Supporting Information

ABSTRACT: There is a growing interest in mediating information transfer between biology and electronics. By the addition of redox mediators to various samples and cells, one can both electronically obtain a redox "portrait" of a biological system and, conversely, program gene expression. Here, we have created a cell-based synthetic biology—electrochemical axis in which engineered cells process molecular cues, producing an output that can be directly recorded via electronics—but without the need for added redox mediators. The process is robust; two key components must act together to provide a valid signal. The system builds on the tyrosinase-mediated conversion of tyrosine to L-DOPA and L-DOPAquinone, which are both redox active. "Catalytic" transducer cells provide for signal-mediated surface expression of tyrosinase.



Additionally, "reagent" transducer cells synthesize and export tyrosine, a substrate for tyrosinase. In cocultures, this system enables real-time electrochemical transduction of cell activating molecular cues. To demonstrate, we eavesdrop on quorum sensing signaling molecules that are secreted by *Pseudomonas aeruginosa*, *N*-(3-oxododecanoyl)-l-homoserine lactone and pyocyanin.

he Internet-of-things has emerged on the basis of transformative developments in our ability to obtain, store, and process information. Its vast networks are a key part of a touted fourth industrial revolution aided by "smart" machine-machine communication. As impactful as they are, these information networks remain largely devoid of biological information. In biological systems, network information is, in part, contained in the structure of its molecules and the transport of its ions. These processes are orthogonal to traditional information transfer in electronics that relies on electrons. We suggest that the redox modality combines features of both electronic and molecular communication and can serve as an effective bridge between biology and electronics. Developments that facilitate biodevice communication, therefore, offer immense promise to monitor and regulate "molecular" communication networks, including those that indicate and control biological function.³⁻⁷ Already, molecular networks have been purposely engineered to yield "smart" metabolic engineering processes, 8-12 synthetic gene regulators, 13-17 and even cell-based therapeutic systems. 18 Electronic connection to these networks will enable user- and machine-guided control.

While many forms of redox communication natively occur in biological networks, ^{23,24} a wide array of metabolically relevant signals are electrochemically inaccessible without added engineering. One approach is to design a biological—electronic interface to transduce information between the two domains.

Specifically, we and others have created biodevice interface systems that enable direct electronic interrogation of native redox communication networks. ^{25,26} Often these function by the addition of redox active mediators that can donate, store, and accept electrons from electrodes. ^{27,28} In a process somewhat analogous to SONAR, redox mediators are "transmitted" by electrodes where they interact with the biological system (e.g., undergo redox reactions) and then return to the electrode where they are "recorded" by measuring current at an applied voltage that is a voltage-based characteristic of the specific mediator. By coupling with data analytics, one can obtain data-rich streams of information. ²⁹

A potent method to expand the "bandwidth" of bioelectronics information transfer, and even reverse the direction of transfer, is to incorporate cells as computational elements in the information pathway. For example, molecular information in biological systems can be interpreted by sensor cells and their transduced signals can be relayed to electrodes as current, again using redox mediators.³⁰ Such living systems can renew

Received: November 21, 2019 Published: March 25, 2020





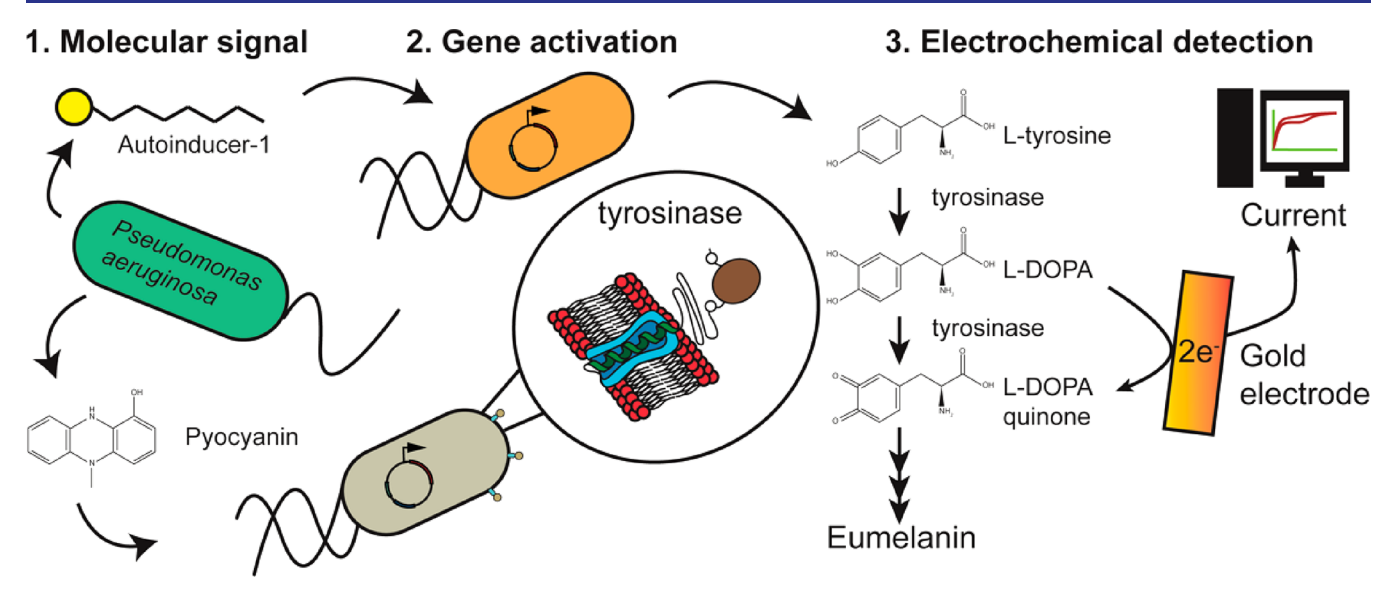


Figure 1. Schematic of the cellular—electronic transduction process. Molecular signals secreted from *Pseudomonas aeruginosa* are detected, integrated, and reported on by direct electronic measurement. One signal, quorum sensing autoinducer-1 (AI-1) serves to coordinate multicellular behavior. Pyocyanin is a phenazine toxin. We have engineered "transducer" *E. coli* cells to convert the "information" that exists by the presence of both of these molecules into an electronic signal. In this way, the molecular communication process that exists in bacterial cultures is electronically relayed via a redox modality. Specifically, "reagent" transducer cells produce L-tyrosine in response to AI-1 (*N*-(3-oxododecanoyl)-l-homoserine lactone). Correspondingly, "catalytic" transducer cells produce an AIDA-tyrosinase fusion, which is localized to their outer membrane surfaces, in response to pyocyanin. Together and only when both signals are present, a coculture of these cells catalyzes the formation of redox molecule L-DOPA from L-tyrosine. L-DOPA is then electronically oxidized to L-DOPAquinone by the presence of a biased gold electrode, generating a current that, in turn, depends on the original concentrations of the biological signaling molecules.

recognition elements without external input and interpret and convey information based on homeostatic context.³¹ Specifically, heterologous genetic circuitry is capable of eavesdropping on molecular communication across various time-scales and reporting back information in a variety of contexts. 30,32-34 To accomplish this form of connectivity, in this work we linked genetic recognition elements of molecular communication signals to the expression of the enzymatic components necessary for the production of the redox active 3,4dihydroxyphenyalanine (L-DOPA) (Figure 1). To do this, we engineered two signal responsive plasmid-based circuits: first, a "reagent" transducer circuit to synthesize L-tyrosine, the natural precursor of L-DOPA, in response to a molecular input; second, a "catalytic" transducer circuit to express tyrosinase on the outer surface of a cell's membrane through an AIDA-linkage. 35,36 L-Tyrosine is a naturally produced aromatic amino acid that undergoes a variety of redox reactions that greatly enhance its electronic activity. 37,38 In particular, tyrosine can be oxidized by the enzyme tyrosinase into the premelanin intermediate, L-DOPA, that can undergo reversible electron exchange between its catecholic and quinone forms. 37-40 This reaction can be interrogated electrochemically to assess tyrosine concentrations and has been exploited for the overproduction of L-DOPA.⁴¹ The overproduction of L-tyrosine and our surface-linked tyrosinase in Escherichia coli are, therefore, an attractive substrate/enzyme pair that couples biological processing to electronics.

That is, we transformed these plasmid-based circuits into separate "catalytic" and "reagent" transducer cells that work together to produce the electronically active L-DOPA signal. Importantly, we designed this coculture system such that, for process robustness, each cell type is needed to establish the bioelectronic connection. Together, the two-cell populations allow for electrochemical eavesdropping on chemical and

bacterial communication networks. We demonstrate the system first by electrochemically interrogating samples containing the redox herbicide, paraquat, and then by eavesdropping on the complex molecular communication network in cultures of *Pseudomonas aeruginosa* by responding to its quorum sensing signal molecule, *N*-(3-oxododecanoyl)-lhomoserine lactone (AI-1) and its phenazine toxin, pyocyanin.

■ MATERIALS AND METHODS

Bacterial Strains and DNA Oligos. Escherichia coli K-12 strain MG1655 (F⁻, λ^- , $ilvG^-$, rfb-50, rph-1, New England Biolabs, Ipswich, MA) was used for amplification of the DNA sequence of soxR and P_{soxRS} . E. coli K-12 strain DH5α (F⁻ φ 80lacZΔM15, Δ (lacZYA argF)U169, recA1, endA1, hsdR17-(r_K^- , m_K^+), phoA, supE44, λ^- , thi-1, gyrA96, relA1, Invitrogen, Carlsbad, CA) was used in all cloning procedures. E. coli K-12 strain 0:17 (Δ ompT, sup+, F^-) was used as template strain for surface expression and tyrosine production. Bacterial strains were stored at -80 °C in 25% (v/v) glycerol (Univar AB, Chicago, IL). All primers were ordered from Integrated DNA technologies (Coralville, IA).

Generation of Gene Knockouts. Single gene knockouts were performed in *E. coli* K-12 strain 0:17 (Δ ompT, sup+, F⁻) as previously described, ⁴² with the modification of the use of nutrient agar supplemented with 50 mM L-rhamnose for removal of the antibiotic gene. The template plasmid used to generate the flippase recognition target flanked *cat* cassettes was plasmid pCmFRT*, ⁴³ a modified version of pKD3⁴⁴ with stop codons replacing either start codons or ribosomal binding sites within the six reading frames of the flippase recognition target sites. Temperature sensitive plasmid pSIJ8⁴² was used for expression of lambda red recombinase and flippase recombinase. The pSIJ8 plasmid was a gift from Alex Nielsen (Addgene plasmid # 68122; http://n2t.net/addgene:68122;

RRID: Addgene_68122). Primers listed in Table S1 were used to generate *cat* fragments resulting in $\Delta tyrR$ and $\Delta soxRS$. Knockouts were confirmed by polymerase chain reaction and sequencing (Eurofin Genomics, Edersberg, Germany) of the resulting DNA fragment (Table S2).

Plasmid Construction. All plasmid assemblies was performed according to Gibson plasmid assembly 45 and restriction-based cloning. All primers, fragments and resulting plasmids are summarized in Tables S3–S4. Heat shock competent $E.\ coli\ DHS\alpha$ were used for initial transformation and screening. Plasmids were verified by sequencing before further use. All enzymes used were from New England Biolabs (NEB) (Ipswitch, MA).

Cultivation Media. Cell propagation for cloning purposes was performed at 37 °C in Lysogeny broth (10 g/L peptone (Merck, Darmstadt, Germany), 5 g/L yeast extract (VWR International, Radnor, PA), 5 g/L NaCl (Scharlau, Barcelona, Spain). Tyrosinase expression experiments were conducted in minimal media (pH = 7.5): 7.0 g/L (NH₄)₂SO₄ (Merck), 3.2 g/L KH₂PO₄ (VWR International), 13.2 g/L Na₂HPO₄· 2H₂O (VWR International), 0.5 g/L (NH₄)₂-H-Citrate (Merck). Prior to cultivation, 1 mL/L of trace element solution, 1 mL/L of 1 M MgSO₄ (Merck), 1 mL/L of 10 mM CuSO₄ (Sigma, St. Louis, MO) were added along with 50 mg/L of targeted antibiotic (chloramphenicol, kanamycin, or ampicillin) (Sigma). The trace element solution contained the following (per liter, all purchased by Sigma): CaCl₂·2H₂O (Sigma), 0.5 g; FeCl₃·6H₂O (Sigma), 16.7 g; ZnSO₄·7H₂O (Sigma), 0.18 g; CuSO₄·5H₂O (Sigma), 0.16 g; MnSO₄·4H₂O (Sigma), 0.15 g; CoCl₂·6H₂O (Sigma), 0.18 g; Na-EDTA (Sigma), 20.1 g. For L-tyrosine production and cocultures, minimal media supplemented with 100 mM of HEPES (Sigma) and 7.5 g/L of glucose (Sigma) (pH = 8.0) was used.

Plate-Based Colorimetric Tyrosinase Activity Assays. Cells were propagated from frozen stocks overnight in minimal media. Cultures were reinoculated in minimal media supplemented with 5 g/L of glucose (Sigma), to an $OD_{600} \approx$ 0.25. Cells were induced at different concentrations of paraquat (PQ) (0.01, 0.05, 0.10, 0.50, 1.00, 5.00 μ M) at an $OD_{600} \approx 0.5$. After 3 h of incubation at 30 °C, cultures were harvested (3000g, 15 min), washed (50 mM Tris-HCl (Sigma), 10 μ M CuSO₄, pH 7.5), and centrifuged again. Resulting pellets were suspended in Tyrosinase assay buffer (1 g/L L-tyrosine (Sigma), 50 mM Tris-HCl, 10 μM CuSO₄, pH 7.5) and incubated at 30 °C. For colorimetric assays, cell solutions were transferred to a 96-well plate and incubated at 30°, in static conditions. After 6 h, plates were centrifuged (2254g, 15 min) and 100 μ L of the supernatant was transferred to a new 96-well plate. The absorbance of each sample was measured at 400 nm with a plate reader (Molecular Devices, San Jose, CA).

Electrochemical Measurement of "Catalytic" Transducer Cell Activation. Catalytic transducer cells were reinoculated from overnight cultures at OD \sim 0.25 in minimal media supplemented with 10 g/L glucose and grown at 37 °C. Cells were induced once the OD reached \sim 0.5 with various concentrations of paraquat (0–2 μM) and pyocyanin from *Pseudomonas aeruginosa* (0–1 μM) (Sigma) and moved to 30 °C for optimal expression. After 4 h, cells were harvested (3000g, 15 min), washed (50 mM Tris-HCl, 10 μM CuSO₄, pH 7.5), and centrifuged again. Resulting pellets were resuspended in Tyrosinase assay buffer and incubated overnight at 30 °C. In the morning (\sim 16 h; 12 h for timed

measurements), 1 mL of cell culture was moved to a glass vial with a fitted cap to position a gold standard electrode (CH Instruments, Austin, TX), a platinum counter wire (Alfa Aesar, Haverhill, MA), and an Ag/AgCl₂ electrode (BASi, West Lafayette, IN). The amount of L-DOPA in solution was then measured using cyclic voltammetry (0–0.55 V, 50 mV/s) using a CH600E or CH1040c electrochemical analyzer (CH Instruments). The L-DOPA oxidation peak was measured to determine peak current between 0.35 and 0.5 V. Experiments employing chronocoulometry were measured by a 30 s pulse at 0.5 V. Three gold electrodes were rotated for all measurements, and electrodes were polished with 0.05 μm diameter silica powder between measurements. If cells were to be remeasured, the samples were returned to the 30 °C incubator for later measurement.

For pulsed-time measurements, cells were grown and washed as described above. Postwashing, cells were resuspended at an $\mathrm{OD}_{600}=3$ in Tyrosinase assay buffer and quickly moved to glass vials preset with a gold standard electrode, a platinum-wire counter, and a $\mathrm{Ag/AgCl_2}$ reference electrode. A CH Instrument macro was then run applying a cyclic voltage wave (0–0.55 V, 50 mV/s) every 15 min for 900 min to four separate samples using a CH1040c multichannel electrochemical analyzer (CH Instruments). All CV files were compiled and the peak currents between 0.35 and 0.5 V were plotted versus time.

Measurement of Pyocyanin Concentration in PA01 P. aeruginosa Conditioned Media. Pseudomonas aeruginosa PA01 cultures were grown overnight in 6 mL of LB, producing a blue-green color as previously reported.⁴⁶ The conditioned media was harvested from the cultures by pelleting out the cellular components (10 000g, 10 min) and filter sterilized with 0.2 μm filters (MilliporeSigma, Burlington, MA). Conditioned media was then serially diluted in LB and added 1:1 with catalytic transducer cells grown in minimal media at $OD_{600} \sim$ 0.5. All tests also included an internal standard of pyocyanin spiked LB to calibrate current measurements. After 4 h of incubation, catalytic transducer cells were harvested, incubated in tyrosinase assay buffer overnight at 30 °C, and analyzed by cyclic voltammetry as described above. Measurements from catalytic transducer cells were compared to the electrochemical measurement of pyocyanin reduction using a gold standard electrode (CH Instruments) as analytically validated and described previously.47,48

Tyrosine Production and Measurement from "Reagent" Transducer Cells. Cells were reinoculated at an $\mathrm{OD}_{600} \sim 0.25$ in 100 mM HEPES minimal media supplemented with 7.5 g/L glucose. Once the cells reached an $\mathrm{OD}_{600} \sim 0.5$, they were induced with various amounts of N-(3-oxododecanoyl)-l-homoserine lactone (Cayman Chemicals, Ann Arbor, MI), referred to as AI-1 in all results and figures for simplicity, and grown at 37 °C for 24 h. The cell supernatant was then harvested (10 000g, 5 min) and mixed 1:1 with potassium phosphate buffer (0.1 M, pH 6.5) and 0.05 mg/L mushroom tyrosinase (EC 1.14.18.1) isolated from Agaricus bisporus (Sigma). Tyrosine amounts were estimated versus an internal standard of tyrosine solutions by measuring the OD_{400} and $\mathrm{OD}_{475/492}$ after 15 min. ³⁶ Values reported in this paper are calculated from the OD_{400} value, which is associated with melanin formation.

Consortia Cultures. Reagent transducer cells (*E. coli* 0:17 $\Delta ompT$, $\Delta tyrR$, $\Delta soxRS$, pAra-Tyrosine, pSox-Tyrosine, or pZS-Las-Tyrosine) were grown overnight in HEPES minimal

media (7.5 g/L of glucose, km or amp) at 37 °C. Reagent transducer cells were reinoculated 1:50 in HEPES minimal media (7.5 g/L of glucose, km or amp) and allowed to grow to an OD_{600} about 0.5 before the addition of inducer molecule. When the reagent transducer cells reached OD_{600} of \sim 5, catalytic transducer cells were added. Catalytic transducer cells (E. coli 0:17 Δ ompT, Δ tyrR, Δ soxRS, pAIDA4Tyr1*0.85) were produced as described above. After 3 h of induction, the cells were harvested (3000g, 15 min) and resuspended in reagent transducer cell cultures to an OD₆₀₀ about 3 (experiment with pAra-Tyrosine) or 5 (experiment with pSox-Tyrosine and pZS-Las-Tyrosine). Hence, the starting OD in the consortia cultures was ~8 (experiment with pAra-Tyrosine) or ~10 (experiment with pSox-Tyrosine and pZS-Las-Tyrosine). The consortia culture was incubated at 30 °C and sampled regularly.

Measurement of Al-1 in Pseudomonas aeruginosa Conditioned Media. Pseudomonas aeruginosa PA01 cultures were grown overnight in 6 mL of LB, producing a blue-green color as previously reported. 46 The conditioned media was harvested from the cultures by pelleting out the cellular components (10 000g, 10 min) and filter sterilized with 0.2 μ m filters (MilliporeSigma, Burlington, MA). AI-1 E. coli reporter cells containing plasmid pAL105⁴⁹ were grown overnight in LB. The conditioned media samples were serially diluted in LB and prepared alongside standard stock solutions of AI-1 (0-60 nM). Ten μ L of each sample was then mixed with 90 μ L of reporter cells and grown at 30 °C for 3 h. The luminescence of each sample tube was then measured using the GloMax-Multi Ir (Promega, Madison, WI, USA) and normalized to the negative control (fresh LB with 0 µM AI-1). The luminescence of the standard curve was then used to estimate the AI-1 content of the conditioned media samples.

Creating Heat Map of Cocultures Exposed to Pyocyanin and Al-1. In order to create a heat map of control reactions, we grew reagent transducer cells ($E.\ coli\ 0:17$ $\Delta ompT,\ \Delta tyrR,\ \Delta soxRS,\ pZS-Las-Tyrosine)$ and catalytic transducer cells ($E.\ coli\ 0:17\ \Delta ompT,\ \Delta tyrR,\ \Delta soxRS,\ pAIDA4Tyr1*0.85)$ as described above. We then added AI-1 and pyocyanin to each culture separately from a premeasured stock. For PA01 conditioned media experiments, we first added the inducers to an equal volume of LB and then added the solution to the culture to account for the excess nutrient supplementation left-over from conditioned media. After induction, the experiment and electrochemical measurements proceeded as described above.

To test the ability of our cell system to transduce molecular information, we first harvested conditioned media from 6 mL of PA01 culture as described earlier. We independently measured AI-1 and pyocyanin as described above. We then diluted the CM in LB 64x to create CM with approximately 1.25 nM and 0.25 μ M, AI-1 and pyocyanin, respectively. This dilution made sure the concentrations of AI-1 and pyocyanin in the diluted CM were within the dynamic range of our coculture system. The experiments then proceeded as described above. The independent measurements were marked on the heat map in Figure 6D by a faded red dot while the result of the cellular transduction of the PA01 signals is marked by the kidney-shaped dashed line.

Experimental Design and Statistics. All experiments were performed in biological triplicates unless otherwise stated. Error bars represent the standard deviation from the mean

value. All linear regressions have an R^2 value of >0.9 and the dotted lines represent the 95% confidence intervals.

■ RESULTS AND DISCUSSION

Electrochemical Detection of L-Tyrosine Oxidation.

The key enzyme to our transduction scheme, tyrosinase, is capable of oxidizing L-tyrosine into the diphenol L-DOPA and the subsequent oxidation of L-DOPA to DOPAquinone. L-DOPA and DOPAquinone can subsequently oligomerize into eumelanin aggregates. Previous work had indicated that the intermediates L-DOPA and leucodopachrome can redox cycle with a biased electrode and thereby generate an electrochemical signal. ^{50,51} In Figure 2A we show how L-tyrosine is

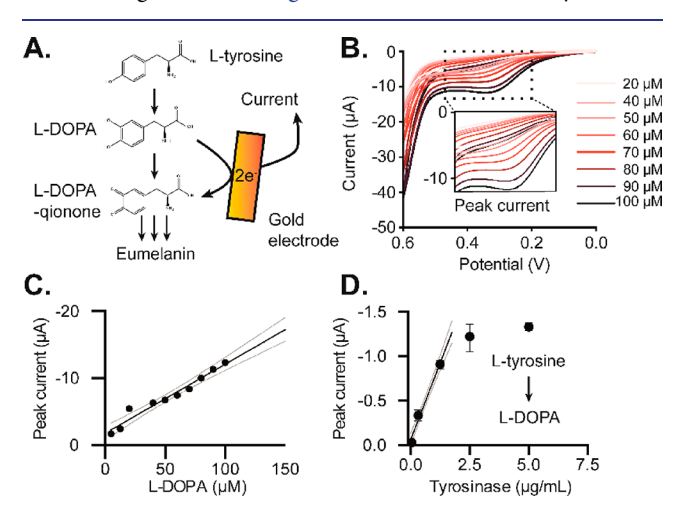


Figure 2. Electrochemical characterization of the enzymatic oxidation of L-tyrosine. (A) Schematic of the enzymatic oxidation of L-tyrosine. L-DOPA and L-DOPAquinone are capable of redox cycling with a gold electrode, generating a measurable electronic signal. (B) Cyclic voltammograms of L-DOPA at various concentrations (20–100 μ M). The zoomed in square depicts the measured current over a range of applied voltages (0.50–0.35 V). (C) The measured peak current is depicted as a function of L-DOPA concentration. (D) The peak current associated with L-DOPA oxidation is found proportional to the concentration of mushroom tyrosinase, the enzyme catalyst of L-DOPA formation from solutions with saturated levels of L-tyrosine.

oxidized (via tyrosinase) to produce L-DOPA, which can then be measured by electronic oxidation to L-DOPAquinone. In Figure 2B, we spiked tyrosine solutions with known concentrations of L-DOPA and applied a cyclic voltage sweep to determine the location of the voltage potentials at which L-DOPA is uniquely oxidized. We found that tyrosine/ eumelanin has minimal oxidative electron transfer between 0 and 0.5 V compared to the oxidation current produced by the conversion of L-DOPA to L-DOPAquinone (Figure 2B). There was no observed overlap with the large tyrosine oxidation peak occurring at ~0.55 V. We plotted the oxidative peak current between 0.35 and 0.5 V from the spiked L-DOPA solutions versus concentration to determine our electrochemical range of detection. We found that the electrochemical signal generated by L-DOPA was concentration dependent between 0 and 100 μ M (Figure 2C). We next added various concentrations of mushroom tyrosinase to saturated L-tyrosine solutions to determine the connection between L-DOPA and enzyme concentration. After ~30 min of incubation, the oxidation peak current between 0.35 and 0.5 V directly correlated to the amount of enzyme added to the solution

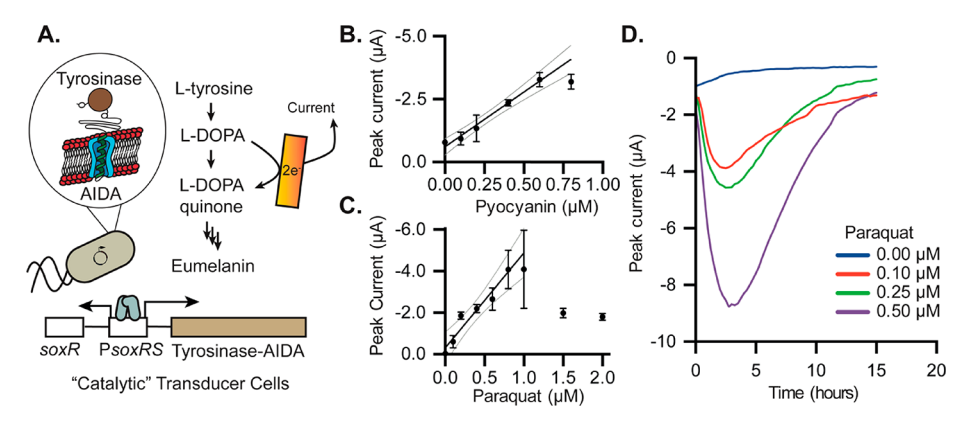


Figure 3. Development of a catalytic transduction system based on the soxRS promoter and surface-displayed tyrosinase. (A) Schematic of the principles of the *Escherichia coli*-based "catalytic" transducer cells. Activation of the soxRS promoter drives expression of an AIDA-tyrosinase fusion. Activated cells with tyrosinase on the outer membrane surface oxidize L-tyrosine to the redox active molecule, L-DOPA. L-DOPA is subsequently oxidized at an electrode surface to L-DOPAquinone. The conversion results in current, which is directly proportional to the original soxRS activator signal, pyocyanin (B) or paraquat (C). (D) The peak current is shown every 15 min for 15 h during experiments with different initial paraquat concentrations.

below 1.25 μ g/mL (Figure 2D). These results indicated that tyrosine and tyrosinase can be coupled to produce a concentration-dependent redox signal that can be accessed between 0.35 and 0.5 V.

Creating a Surface-Displayed Tyrosinase "Catalytic" Cell Population. We next aimed to connect the tyrosinetyrosinase electrochemical couple to genetic circuitry in E. coli "catalytic" transducer cells. To do this, we used the bidirectional soxRS promoter system for driving tyrosinase expression and the AIDA transporter for translocation to the outer surface of the cell. The soxRS promoter has previously been used to detect herbicides (e.g., diquat, dicamba, paraquat) and redox toxins (e.g., pyocyanin). 30,52-54 Specifically, we coupled this promoter system to the previously developed tyrosinase vector, 35,36 creating the plasmid pAIDA2Tyr10.85. We theorized that surface expression of the tyrosinase-AIDA fusion would expose the tyrosinase to extracellular tyrosine and copper cofactors thus decreasing the need for cell membrane transporters that would be required for import/export of the impermeable components (Figure 3A). We also introduced a point mutation (V284G) to the tyrosinase sequence as this had previously been shown to increase the enzymatic formation of L-DOPA.55 Together, these features link soxS promoter activation by molecular signals to the number of AIDA-tyrosinase fusion constructs on the surface of the cell, and ultimately increased enzymatic activity. To test the plasmid system, we induced the expression of the surface-displayed tyrosinase with paraquat and immersed the cells in tyrosine-containing solutions at varying cell densities. We then measured the optical signal at 400 nm of each sample over time to determine the extent of eumelanin formation, which follows the production of L-DOPA. That is, eumelanin has broad-spectrum absorbance and has previously been quantified by measuring absorbance at 400 nm.³⁶ We observed that the optical signal increased both with tyrosine concentration and cell-density (Figure S1). These results indicated that the catalytic transducer cells were producing L-DOPA relative to the amount of enzyme and tyrosine present in the system.

We next tested the concentration-dependence of transcriptional regulation of the surface-expressed tyrosinase when the cells were induced with varying concentrations of paraquat and

pyocyanin. Induced cells were incubated at 30 °C in a saturated L-tyrosine solution and the L-DOPA concentration was measured using cyclic voltammetry. We found that the catalytic transducer cells produced inducer-dependent oxidative peak currents between 0.35 and 0.5 V (pyocyanin Figure 3B; paraquat Figure 3C). We note that the signal decrease above 1.0 µM paraquat is a result of cell death (data not shown), in keeping with observations from prior work.⁵⁶ In control tests without tyrosine or prior to induction, oxidative peaks could not be detected (Figure 3B,C; Figure S2). To determine the dynamics of our system, we induced our cells as previously described and, upon introduction to a saturated Ltyrosine solution, we measured the oxidative peak currents by cyclic voltammetry every 15 min. The cell-densities for each sample were fixed at an OD_{600} of 3 to correct for the growth rate retardation caused by inducer toxicity (data not shown), consistent with previous studies.⁵³ We observed concentration dependent oxidative peak currents within ~2 h (Figure 3D). To determine the influence of surface-expression, we repeated this experiment with both an AIDA-linked tyrosinase and a parallel cytosolic tyrosinase expression system. Importantly, we found that only surface-expressed tyrosinase produced redox signals within the ~16-h time period post induction (Figure S3). These results indicated that the catalytic transducer cells produced inducer concentration-dependent electrochemical signals. The peak currents were consistent with tyrosineoxidation and the signal was relatively stable, as was indicated by inducer-dependent measurements measured post overnight incubation. Interestingly, however, the overnight samples in Figure 3B, though still concentration-dependent, exhibited lower values than the inducer-dependent peak currents measured during the 15 min electronic pulses presented in Figure 3D, suggesting overnight depletion of L-DOPA components. Our initial OD measurements in Figure S1 indicated eumelanin formation was similarly concentration dependent on tyrosine, cell density, and paraquat. One possible explanation for the loss of signal in overnight samples could be depletion of L-DOPA components due to eumelanin formation.⁵⁷ Prior work has indicated that eumelaninformation from mushroom tyrosinase could deplete electroactive pools, albeit at different rates. 50 After additional testing (data not shown) we concluded instead that a significant

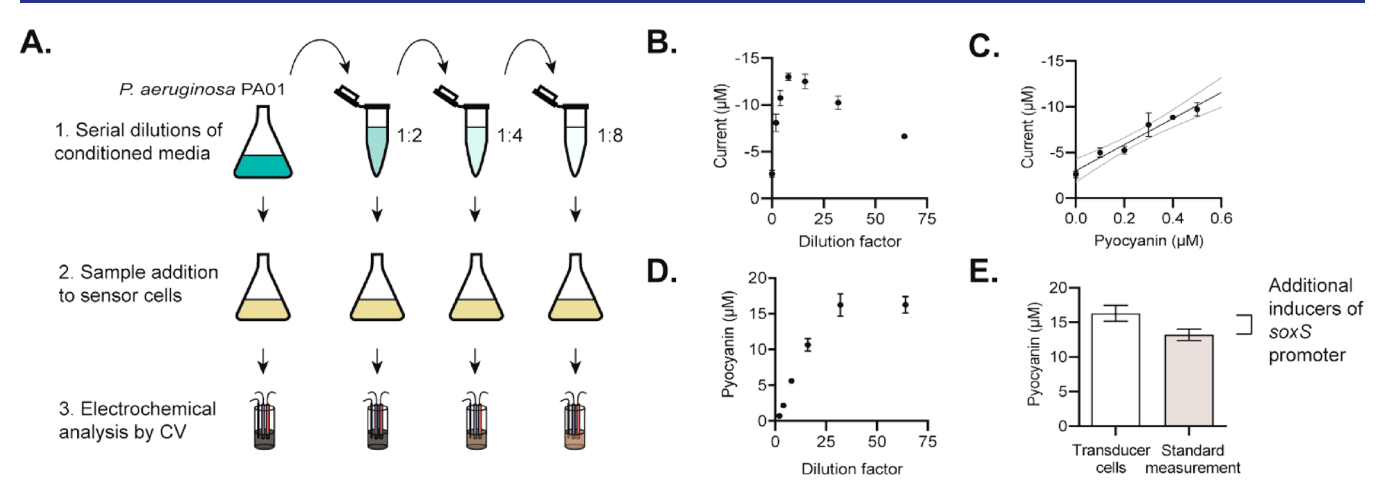


Figure 4. Characterization of a *Pseudomonas aeruginosa* supernatant (PA01) by the catalytic transducer cells. (A) Schematic representation of the methodology used to characterize PA01 conditioned media (CM). CM was serially diluted (i.e., 1/2 dilution increments) in fresh LB, then added to catalytic transducer cell cultures. Current measurements were made after overnight incubation in a saturated tyrosine buffer. (B) Current measurements from the catalytic transducer cells at different dilutions of the original PA01 CM sample. (C) Current measurements from the catalytic transducer cell assay in response to known concentrations of pyocyanin suspended in LB. (D) Estimated pyocyanin concentration measured from serially diluted samples; dilution reduces confounding molecular interference. (E) A comparison of the pyocyanin level indicated by catalytic transducer cells compared to an independent electrochemical measurement. Comparison of each measurement revealed a consistent \sim 3.0 μ M offset in pyocyanin level between the transducer cell assay and the independent electrochemical measurement. This was consistent with the calculated offset from spiking conditioned media with known concentrations of pyocyanin (Figure S4).

fraction of the decrease in current in Figure 3D post ~2 h was caused by electrode fouling from phenolic components, a common problem in phenol electrochemistry, ⁵⁸ as the currents had dropped below measurements taken of overnight incubation samples, but with clean electrodes. In sum, our data presented in Figure 3 shows that expression of a surface-linked tyrosinase can be actuated in an inducer dose-dependent manner and that electrochemically active signals can be generated by exposing the induced cells to L-tyrosine. In addition, the peak currents are formed rapidly after the L-tyrosine and tyrosinase are placed in contact with each other. Moreover, the signals generated persisted, albeit at lower values, for nearly a day after initial exposure.

Catalytic Transducer Cell Evaluation of Pyocyanin within Pseudomonas Secretome. To evaluate the ability of our catalytic transducer cells to interpret molecular signals within complex solutions, we incubated the cells with conditioned media from cultures of Pseudomonas aeruginosa. Virulent strains of Pseudomonas aeruginosa, such as PA01,46 secrete redox active compounds during phosphate-limited, hypoxic growth.⁵⁹ Among these compounds, pyocyanin is a toxin typically secreted late in the growth phase due to earlier accumulation of quorum sensing signals, acyl homoserine lactones (AHLs). First, we harvested conditioned media from PA01 cells grown in LB media overnight, we next serially diluted the media with fresh LB, and then added the diluted conditioned media (CM) to our catalytic transducer cells to induce tyrosinase expression (Figure 4A). The cells were then pelleted and assayed with tyrosinase buffer for L-DOPA formation by cyclic voltammetry as previously described. We performed serial dilutions to ensure the amount of pyocyanin used to induce the catalytic transducer cells did not cause significant toxicity or saturate the tyrosinase expression of the cell. In parallel, we added known concentrations of pyocyanin into fresh LB and added the media to catalytic transducer cell cultures to mimic the Pseudomonas CM tests, but that omit other secreted products. In this way, we constructed a pyocyanin/current calibration curve specific to the experimental conditions. We found low current levels in undiluted CM and these levels increased with dilution until a dilution factor of 8x, after which the current decreased with increasing dilution (Figure 4B). We note, however, the apparent pyocyanin concentration, which was calculated using the calibration curve and the dilution factor (Figure 4C), increased with dilution until 32×, suggesting that ill-defined components that attenuate the cell response were being diluted out. Then, that at larger dilutions the apparent concentration dropped and by comparison to the controls (not shown here), only the pyocyanin contributed to the cell response (Figure 4D). In sum, the pyocyanin level in CM was found to be 16.3 μ M. Interestingly, our measurements were also consistent with our previous findings that the induction of tyrosinase became saturated at $\sim 0.5 \mu M$ pyocyanin, which was the approximate amount of pyocyanin in the 32× dilution, as seen in Figure 3B.

Then, in order to compare our technique to an acellular method, we used cyclic voltammetry to measure the directelectron transfer of pyocyanin, indicated by its peak reductive current at ~ -0.25 V, from the same conditioned media.⁴⁷ Electrochemical detection has been previously verified as a robust analytical detection method for phenazines secreted by P. aeruginosa. 48 Again, based on calibration curves, we found the CM contained 13.2 μ M pyocyanin. This was ~3.0 μ M less than that measured by the catalytic transducer cell assay (Figure 4E) and, importantly, was statistically significant (pvalue 0.019). We hypothesized that the difference was due to the presence of alternative SoxRS inducer molecules (e.g., phenazine-1-carboxylic acid⁶⁰) within the *P. aeruginosa* secretome. To gain additional insight into the presence of additional oxidative species, we spiked serially diluted CM with additional pyocyanin and subtracted the measured standard from the samples. Using this methodology, we found these contributing and unidentified molecules were present at a 4.8 μM "pyocyanin equivalent" (Figure S4). Interestingly, this roughly coincides with the measurement gap in Figure 4E. Together, these data suggest soxRS activation and the use of cellular reporting methodologies can provide additional insight into

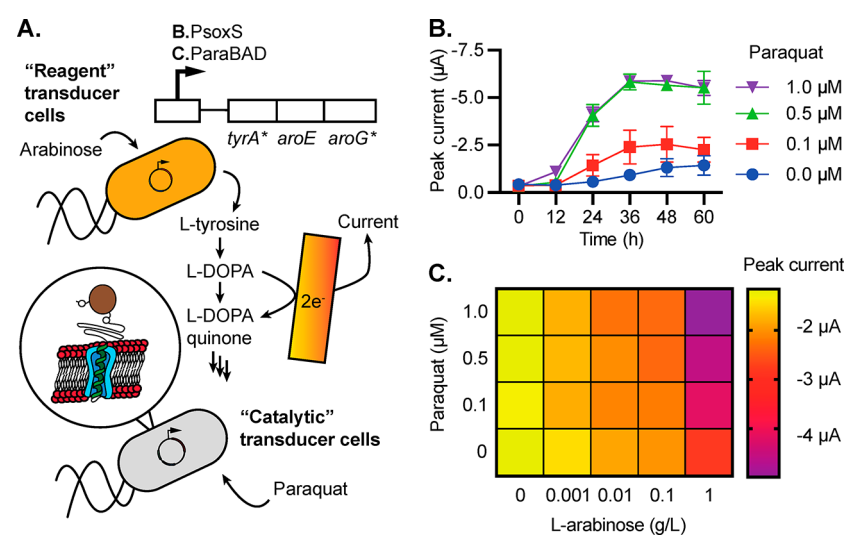


Figure 5. Coculture system comprised of "catalytic" and "reagent" transducer cells. (A) Schematic of the coculture. This system relies on "reagent" transducer cells to generate L-tyrosine by signal-activated overexpression of the genes $tyrA^*$, aroE, and $aroG^*$. The "catalytic" transducer cells express tyrosinase on their outer surfaces after activation of the psoxS promoter via paraquat (B) or after activation of the araBAD promoter by the addition of arabinose (C). Also, in (C), a heat map is generated showing the peak currents after coculture of catalytic and reagent cells were exposed to known concentrations of activator signals.

the biological context of redox active signals. Specifically, such cellular "computation" serves to integrate the oxidative activity or potentially toxicological information present in complex CM samples, beyond that of the readily apparent phenazine toxin, pyocyanin.

Molecular to Electronic Information Transfer by Mediator-Independent Coculture. Next, in order to generate a robust bio-to-electronic information circuit that is less subject to cell variability, we extended our cellular computation scheme by creating a dual plasmid format that integrates signal specific expression of tyrosinase with signal directed cellular production of tyrosine. In this way, two data streams, each with an intrinsic level of uncertainty must be combined in a specific way to generate a positive response. The requirement for both circuits to be activated is analogous to an AND logic gate, with L-DOPA oxidation to L-DOPAquinone only occurring when both tyrosine is produced and tyrosinase is expressed on the cell surface. Building upon existing literature for tyrosine overproduction, 61,62 we developed vectors for expressing feedback resistant tyrA* and aroG* alongside aroE to catalyze key steps in tyrosine biosynthesis. Two variants of tyrosine producing plasmids were assembled to test this concept: the first, pAra-Tyrosine, where the 3 tyrosine-associated enzymes were regulated by two ara_{BAD} promoters; and the second, pSox-Tyrosine, where the same enzymes were regulated by a single soxRS promoter system having computationally optimized ribosomal binding sites (~90%).⁶³ These two constructs were separately transformed into an E. coli 0:17 \(\Delta tyrR \) \(\Delta soxRS \) mutant strain to create tyrosine "reagent" transducer cells. These transducer cells were induced with varying levels of either arabinose (for pAra-Tyrosine) or paraquat (for pSox-Tyrosine) and grown 24 h at 37 °C in ~7.5 g/L glucose media. Cells expressing pAra-Tyrosine showed inducer concentration dependent production of tyrosine when titrated with arabinose. Cells produced up to \sim 1 g/L tyrosine post 24 h of expression (Figure S5). There was, however, no paraquat-dependent regulation from cells expressing pSox-Tyrosine at levels of paraquat tested. Instead, these cells produced ~1 g/L tyrosine even without paraquat

induction as measured 24 h postinduction. Owing to its simplicity, we decided to use the strain containing pSox-Tyrosine when we wanted constitutive L-tyrosine production.

To couple the expression of tyrosinase with the production of tyrosine, we developed two systems. We transformed the plasmids into a single cell and also into two-separate populations comprising a coculture. In the single cell case, L-DOPA was formed as expected but the yields were low and inconsistent (data not shown). Perhaps, this was a case in which our desired function overburdened the redirection capacity of a single cell. 64-66 Instead, we focused our efforts on the coculture system wherein each plasmid of an AND logic gate was expressed in separate "catalytic" and "reagent" cell populations (Figure 5A). To test the ability of our cell network to produce an L-DOPA signal, we incubated a coculture of pSox-Tyrosine reagent transducer cells and tyrosinase-expressing catalytic transducer cells with varying amounts of paraquat and periodically measured the L-DOPA signal in the conditioned media with cyclic voltammetry. We found that the oxidative peak current produced by our coculture system for the first 12 h was dependent on the amount of paraquat $(0-0.5 \mu M)$ added to induce tyrosinase in the catalytic transducer cell population (Figure 5B). These results were consistent with stepped oxidative pulses for both constitutive and regulated tyrosine production (Figure S6A). Importantly, the differences in current remained stable for up to 60 h (Figure 5B). On the basis of these experiments, we analyzed several coculture experiments at 24 h postmixing.

Specifically, we next tested the integration of multiple molecular signals into a single electronic output by separately inducing the catalytic and reagent transducer cell populations. To the reagent transducer population harboring the arabinose inducible promoter (pAra-Tyrosine), we added arabinose (0–1 g/L) and grew the cells to an OD of \sim 5. We then mixed these cells with pelleted catalytic transducer cells that had been preinduced with paraquat (0–1 μ M) such that the final catalytic transducer population was approximately OD 3. After 24 h of incubation, we observed that the peak currents increased with both arabinose and paraquat concentrations

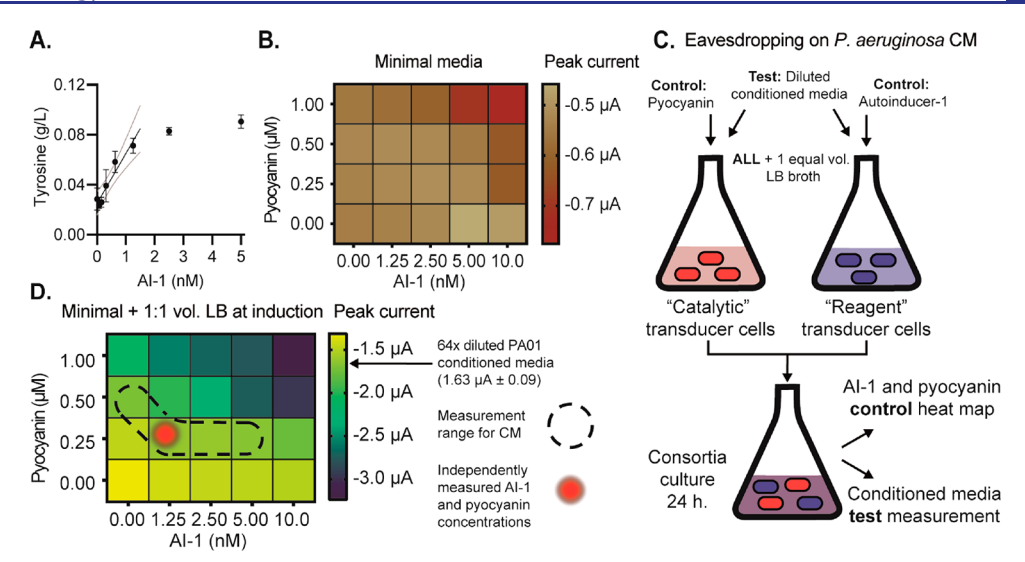


Figure 6. Cocultures analyzing the *Pseudomonas* quorum sensing signals pyocyanin and autoinducer-1. (A) L-tyrosine production from reagent transducer cells in response to *N*-(3-oxododecanoyl)-l-homoserine lactone (AI-1). (B) Heat map of coculture generated peak current as a function of both pyocyanin and AI-1 concentrations. Cells suspended in 10 mL 100 mM HEPES minimal media were supplemented with known concentrations of signal molecules similar to Figure 5C. (C) Schematic of the coculture experiments using *Pseudomonas aeruginosa* (strain PA01) conditioned medium (CM). Catalytic and reagent transducer cultures grown in HEPES minimal media were first induced with known concentrations of pyocyanin or AI-1 dissolved in LB medium. This recapitulates the heat map of (B) but allows for comparison to PA01 CM, which contains residual LB. Then, PA01 CM was diluted with LB as in Figure 4 to dilute the secreted AI-1 and pyocyanin concentrations into the linear response range of both cell populations. The diluted CM was then incubated with cocultures for 24 h to evaluate electronic output as a function of the secreted signal molecules. (D) Peak currents from known concentrations are displayed as a control heat map. Overall, currents were higher than (B) due to the addition of LB media (i.e., cell responses are amplified in LB). The independently measured concentrations of both AI-1 and pyocyanin in the PA01 CM is depicted by the red dot. In concordance, the dashed line region represents the current generated by the coculture treated with CM.

(Figure 5C, Figure S7A). Arabinose significantly increased the amount of current measured by cyclic voltammetry, and we found the influence of paraquat had the most impact when the reagent cells had been treated with 1 g/L arabinose ($-2.8~\mu V$ to $-5.0~\mu V$, Figure 5C, Figure S7A). We observed similar trends when measuring output via chronocoulometry (Figure S6B, Figure S7B). These results indicated that the two biological inputs, arabinose and paraquat, could be integrated by a mixture of cells into a single electronic output.

Next, we altered our coculture system to eavesdrop on the cell-cell communication of Pseudomonas aeruginosa (PA). These bacteria and many others coordinate their behaviors by secreting and detecting autoinducer signaling molecules in a widely recognized process called quorum sensing.⁶⁷ Specifically, PA cells signal to each other via acyl homoserine lactones, including N-(3-oxododecanoyl)-l-homoserine lactone autoinducer-1 (AI-1) and they subsequently produce the toxin pyocyanin at higher cell densities. In Figure 6, in a similar manner to treatments with arabinose and paraquat shown in Figure 5, we provided these signals to cells engineered to respond by making either tyrosine or tyrosinase. To do this, we first constructed a plasmid for AI-1 dependent tyrosine production by exchanging the arabinose promoter and repressor for the luxI promoter and LasR transcriptional activator from a previously engineered GFP construct.⁶⁸ We then moved the promoter and coding region to the plasmid pZS*luc13 with a pSC101* origin and evaluated AI-1dependent tyrosine production after 24 h growth in 7.5 g/L glucose. The low-copy construct produced between ~0.03-0.1 g/L tyrosine in response to AI-1 (0-5 nM) (Figure 6A). Using this reagent transducer variant, pZS-Las-Tyrosine, we evaluated the ability of a mixed coculture using AI-1 and

pyocyanin-sensitive catalytic transducer cells to simultaneously evaluate both of the quorum sensing inputs. Together, these cells produced an input-dependent change in oxidative peak current (-0.55 to $-0.78~\mu\text{A}$) in response to both AI-1 and pyocyanin (0-10~nM and $0-1~\mu\text{M}$ respectively; Figure 6B, Figure S8A). Results are illustrated in a heat map showing the amalgamation of many experiments covering a wide range of concentrations. Analogously to Figure 5, results indicate that the coculture system successfully integrates two molecular signals into a single electrical output. Importantly, this function proceeds based on the coupling of cell-based recognition and signal transduction that is transmitted directly to electronically observed signals. There is no need for exogenous redox mediators, just a nearby biased electrode.

Finally, we tested the ability of the reagent and catalytic transducer cells to determine the quantities of each quorum sensing signal in conditioned medium after growth of P. aeruginosa (see scheme in Figure 6C). That is, we tested whether the cell coculture could be used to recognize independent signals secreted by cells, integrate this information, and then provide an electronic output that in turn might approximate the relative levels of each signal. In this way, the system could be used to gauge additional insight regarding the presence of the pathogen. We first developed a control heat map, analogously to that above. AI-1 and pyocyanin were first added to LB medium, because LB was later used to culture PA cells and from which CM was obtained. The LB containing pyocyanin or AI-1 (10 mL) was added to an equal volume of transducer cells that had been reinoculated and grown to mid log phase in 100 mM HEPEs minimal media. The presence of LB when inducing the cells resulted in greater L-DOPA peak currents when compared to our previous tests (-1.3 to -3.2)

 μ A compared to -0.55 to -0.78 μ A, Figure 6B,D, Figure S8). Using this methodology, we quantified the current output as a function of both AI-1 and pyocyanin concentration.

We next grew the PA01 cells in 6 mL of LB medium and independently measured the quantities of the signal molecules (see Materials and Methods). We have marked these on the heat map by a red dot (Figure 6D). In this way, we establish an expectation for the current obtained by the coculture exposed to the PA CM. That is, to evaluate the electronic transduction of the molecular communication in P. aeruginosa CM, we added the diluted CM to separate, mid log growth cultures of catalytic and reagent transducer cells at a 1:1 volume ratio. Following the creation of the heat map, a 10 mL culture of transducer cells growing in 100 mM HEPEs minimal media would be induced with 10 mL CM (diluted in LB so that samples were in the linear range, see Materials and Methods). After 24 h, we measured the oxidative peak current and found a value of 1.63 \pm 0.09 μ A. On Figure 6D, we have highlighted the areas of the heat map that correspond to that current by the kidney shaped dotted line. We note that this area covers regions of 0.25 µM pyocyanin and from 0 to 5 nM AI-1. As indicated by the faded red dot on the heat map, our independent measurements revealed that the concentrations of AI-1 and pyocyanin were 0.25 μ M and 1.25 nM. Accordingly, the engineered coculture accurately communicated both the AI-1 and pyocyanin concentrations that had been naturally secreted into the CM by P. aeruginosa.

This cell-based electrochemical reporter system is unique in that it produces a strong redox signal through the production of tyrosinase and its substrate tyrosine without the need for external mediators. The produced tyrosine is oxidized by surface-expressed tyrosinase to L-DOPA, which has a distinct electrochemical potential. This dual regulation allows for the integration of gene-circuits by transcriptional regulation of the enzymatic components. Using this regulation, our catalytic transducer cell population was able to detect various concentrations of soxRS activating substances. This information, in turn, was used to measure the pyocyanin content of conditioned media from the opportunistic pathogen Pseudomonas aeruginosa. Furthermore, we demonstrated that this reporting system can be split between two-cell populations, illustrating the ability of network computation to integrate molecular communication. This feature provides for robust computation in that a positive signal is not generated without the independent input of two cell types. If a single engineered sensor cell were used, a spurious false positive could more readily occur. Further, we showed that the system is adaptable and can report on various inducer signals, which we demonstrated by eavesdropping on the communication signals AI-1 and pyocyanin, either independently or from Pseudomonas aeruginosa conditioned media, as well as signals from environmental or bioprocessing environments, paraquat and arabinose, respectively.

We suggest that this redox-based output system could be extended to compute further molecular communication signals. Tyrosinase is a promiscuous enzyme, able to display monophenolase and biphenolase activity on diverse phenolic-like substances ^{69,70} including dopamine ⁷¹ and bisphenol A. ^{72,73} Future applications of this form of cellular communication might utilize a range of substrates and the various products might be detected at different voltages, or on different electrodes where different reagent transducer cells are located. The use of tyrosinase also allows integration with various

metabolic pathways relevant to biotechnology beyond tyrosine, including opiates, 74 alkaloids, 75,76 and melanins. 62,77 This system can also be integrated with responsive electrode films, to both enhance computational capacity and reduce phenolic fouling. 78

We believe future applications of this technology will take advantage of the advanced processing abilities of cell populations. The use of two cell populations allows for unique information processing as compared to monocultures.⁷⁹ The use of cell consortia allows for divisions of labor to lower any particular metabolic burden as well as the creation of plug-andplay strains that might be mixed as needed. 80 Our coculture system might also be used to create an OR type logic gate by similar strategies as we have presented in Figure 5B. Alternatively, such cocultures might be used as a communication portal to enable external control systems in combination with electronic "controller" populations. Examples of these systems include "controller" cell populations that relay electronic commands to molecular signals to modulate population densities to meet user-specified objectives, as has previously been explored with guided metabolite usage, bacterial chemotaxis, and myocyte contraction. 52,81 Combination of "controller" populations with our coculture transduction system would allow for closed-loop applications with the potential for active user-mediated intervention to oversee completion of the task—as indicated by cellular current generation. Finally, because the redox-based output is directly detected as current under an applied voltage without any additional mediators, and the cells remain intact through the assay, this system will open the networking capabilities of biological information into the greater Internet-of-things and thereby advance the research fields of biological-electronic information transfer.

ASSOCIATED CONTENT

Supporting Information

The Supporting Information is available free of charge at https://pubs.acs.org/doi/10.1021/acssynbio.9b00469.

Sequence of all primers and cloning details for all plasmids generated in this work, optical measurements of tyrosinase activity, control cyclic voltammograms, comparisons between cytosolic and surface-expressed tyrosinase "catalytic" transducer cell activity, measurement of nonpyocyanin inducers of "catalytic" transducer cells and the AI-1 content of *P. aeruginosa* conditioned media, and scatterplot representations of data from Figure 5 and Figure 6 (PDF)

AUTHOR INFORMATION

Corresponding Author

William E. Bentley — Fischell Department of Bioengineering, University of Maryland, College Park, Maryland 20742, United States; orcid.org/0000-0002-4855-7866; Email: bentley@ umd.edu

Authors

Eric VanArsdale — Fischell Department of Bioengineering, University of Maryland, College Park, Maryland 20742, United States

David Hörnström — Department of Industrial Biotechnology, School of Engineering Sciences in Chemistry, Biotechnology and

- Health, KTH Royal Institute of Technology, AlbaNova University Center, SE 10691 Stockholm, Sweden
- Gustav Sjöberg Department of Industrial Biotechnology, School of Engineering Sciences in Chemistry, Biotechnology and Health, KTH Royal Institute of Technology, AlbaNova University Center, SE 10691 Stockholm, Sweden
- Ida Järbur Department of Industrial Biotechnology, School of Engineering Sciences in Chemistry, Biotechnology and Health, KTH Royal Institute of Technology, AlbaNova University Center, SE 10691 Stockholm, Sweden
- Juliana Pitzer Fischell Department of Bioengineering, University of Maryland, College Park, Maryland 20742, United States
- Gregory F. Payne Fischell Department of Bioengineering, University of Maryland, College Park, Maryland 20742, United States; Ocid.org/0000-0001-6638-9459
- Antonius J. A. van Maris Department of Industrial Biotechnology, School of Engineering Sciences in Chemistry, Biotechnology and Health, KTH Royal Institute of Technology, AlbaNova University Center, SE 10691 Stockholm, Sweden

Complete contact information is available at: https://pubs.acs.org/10.1021/acssynbio.9b00469

Author Contributions

§E.V.A. and D.H. contributed equally to this work.

Notes

The authors declare no competing financial interest.

ACKNOWLEDGMENTS

Thanks to Alex Nielsen for the pSIJ8 (Addgene plasmid #68122). Partial support of this work was provided by DTRA (HDTRA1-19-0021), NSF (DMREF #1435957, ECCS#1807604, ECCS#1809436, ECCS#1926793, CBET#1805274), and the National Institutes of Health (R21EB024102). D.H. was funded by grant VR-621-2014-5293 from the Swedish Research council (VR). G.S. additionally received funding from the Swedish research council Formas (211-2013-70).

■ REFERENCES

- (1) Akyildiz, I., Pierobon, M., Balasubramaniam, S., and Koucheryavy, Y. (2015) The Internet of Bio-Nano Things. *IEEE Commun. Mag.* 53 (3), 32–40.
- (2) Kim, E., Li, J., Kang, M., Kelly, D. L., Chen, S., Napolitano, A., Panzella, L., Shi, X., Yan, K., Wu, S., et al. (2019) Redox Is a Global Biodevice Information Processing Modality. *Proc. IEEE 107* (7), 1402–1424.
- (3) Liu, Y., Li, J., Tschirhart, T., Terrell, J. L., Kim, E., Tsao, C.-Y., Kelly, D. L., Bentley, W. E., and Payne, G. F. (2017) Connecting Biology to Electronics: Molecular Communication via Redox Modality. *Adv. Healthcare Mater.* 6 (24), 1700789.
- (4) Feiner, R., and Dvir, T. (2018) Tissue–Electronics Interfaces: From Implantable Devices to Engineered Tissues. *Nat. Rev. Mater.* 3 (1), 17076.
- (5) Li, J., Wu, S., Kim, E., Yan, K., Liu, H., Liu, C., Dong, H., Qu, X., Shi, X., Shen, J., et al. (2019) Electrobiofabrication: Electrically Based Fabrication with Biologically Derived Materials. *Biofabrication* 11 (3), 032002.
- (6) Milias-Argeitis, A., Rullan, M., Aoki, S. K., Buchmann, P., and Khammash, M. (2016) Automated Optogenetic Feedback Control for Precise and Robust Regulation of Gene Expression and Cell Growth. *Nat. Commun.* 7 (1), 12546.
- (7) Terrell, J. L., Wu, H.-C., Tsao, C.-Y., Barber, N. B., Servinsky, M. D., Payne, G. F., and Bentley, W. E. (2015) Nano-Guided Cell

- Networks as Conveyors of Molecular Communication. *Nat. Commun.* 6 (1), 8500.
- (8) You, L., Cox, R. S., Weiss, R., and Arnold, F. H. (2004) Programmed Population Control by Cell–Cell Communication and Regulated Killing. *Nature* 428 (6985), 868–871.
- (9) Xu, P. (2018) Production of Chemicals Using Dynamic Control of Metabolic Fluxes. *Curr. Opin. Biotechnol.* 53, 12–19.
- (10) Jones, J. A., and Wang, X. (2018) Use of Bacterial Co-Cultures for the Efficient Production of Chemicals. *Curr. Opin. Biotechnol.* 53, 33–38.
- (11) He, F., Murabito, E., and Westerhoff, H. V. (2016) Synthetic Biology and Regulatory Networks: Where Metabolic Systems Biology Meets Control Engineering. *J. R. Soc., Interface* 13 (117), 20151046.
- (12) Gupta, A., Reizman, I. M. B., Reisch, C. R., and Prather, K. L. J. (2017) Dynamic Regulation of Metabolic Flux in Engineered Bacteria Using a Pathway-Independent Quorum-Sensing Circuit. *Nat. Biotechnol.* 35 (3), 273–279.
- (13) Niederholtmeyer, H., Chaggan, C., and Devaraj, N. K. (2018) Communication and Quorum Sensing in Non-Living Mimics of Eukaryotic Cells. *Nat. Commun.* 9 (1), 5027.
- (14) Sedlmayer, F., Hell, D., Müller, M., Ausländer, D., and Fussenegger, M. (2018) Designer Cells Programming Quorum-Sensing Interference with Microbes. *Nat. Commun.* 9 (1), 1822.
- (15) Tekel, S. J., Smith, C. L., Lopez, B., Mani, A., Connot, C., Livingstone, X., and Haynes, K. A. (2019) Engineered Orthogonal Quorum Sensing Systems for Synthetic Gene Regulation in Escherichia Coli. *Front. Bioeng. Biotechnol.* 7 (April), 1–12.
- (16) Danino, T., Mondragón-Palomino, O., Tsimring, L., and Hasty, J. (2010) A Synchronized Quorum of Genetic Clocks. *Nature* 463 (7279), 326–330.
- (17) Butzin, N. C., Hochendoner, P., Ogle, C. T., and Mather, W. H. (2017) Entrainment of a Bacterial Synthetic Gene Oscillator through Proteolytic Queueing. *ACS Synth. Biol.* 6 (3), 455–462.
- (18) Tsao, C.-Y., Quan, D. N., and Bentley, W. E. (2012) Development of the Quorum Sensing Biotechnological Toolbox. *Curr. Opin. Chem. Eng.* 1 (4), 396–402.
- (19) Virgile, C., Hauk, P., Wu, H.-C., Shang, W., Tsao, C.-Y., Payne, G. F., and Bentley, W. E. (2018) Engineering Bacterial Motility towards Hydrogen-Peroxide. *PLoS One* 13 (5), No. e0196999.
- (20) McKay, R., Hauk, P., Wu, H.-C., Pottash, A. E., Shang, W., Terrell, J., Payne, G. F., and Bentley, W. E. (2017) Controlling Localization of Escherichia Coli Populations Using a Two-Part Synthetic Motility Circuit: An Accelerator and Brake. *Biotechnol. Bioeng.* 114 (12), 2883–2895.
- (21) Wu, H., Tsao, C., Quan, D. N., Cheng, Y., Servinsky, M. D., Carter, K. K., Jee, K. J., Terrell, J. L., Zargar, A., Rubloff, G. W., et al. (2013) Autonomous Bacterial Localization and Gene Expression Based on Nearby Cell Receptor Density. *Mol. Syst. Biol.* 9 (1), 636.
- (22) McKay, R., Hauk, P., Quan, D., and Bentley, W. E. (2018) Development of Cell-Based Sentinels for Nitric Oxide: Ensuring Marker Expression and Unimodality. *ACS Synth. Biol.* 7 (7), 1694–1701.
- (23) Go, Y.-M., and Jones, D. P. (2013) The Redox Proteome. J. Biol. Chem. 288 (37), 26512-26520.
- (24) Antunes, F., and Brito, P. M. (2017) Quantitative Biology of Hydrogen Peroxide Signaling. *Redox Biol.* 13 (April), 1–7.
- (25) Kim, E., Leverage, W. T., Liu, Y., White, I. M., Bentley, W. E., and Payne, G. F. (2014) Redox-Capacitor to Connect Electrochemistry to Redox-Biology. *Analyst* 139 (1), 32–43.
- (26) Liu, Y., Kim, E., Li, J., Kang, M., Bentley, W. E., and Payne, G. F. (2017) Electrochemistry for Bio-Device Molecular Communication: The Potential to Characterize, Analyze and Actuate Biological Systems. *Nano Commun. Netw.* 11, 76–89.
- (27) Kim, E., Liu, Z., Liu, Y., Bentley, W., and Payne, G. (2017) Catechol-Based Hydrogel for Chemical Information Processing. *Biomimetics* 2 (3), 11.
- (28) Kang, M., Kim, E., Temoçin, Z., Li, J., Dadachova, E., Wang, Z., Panzella, L., Napolitano, A., Bentley, W. E., and Payne, G. F. (2018) Reverse Engineering To Characterize Redox Properties: Revealing

- Melanin's Redox Activity through Mediated Electrochemical Probing. Chem. Mater. 30 (17), 5814–5826.
- (29) Kang, M., Kim, E., Chen, S., Bentley, W. E., Kelly, D. L., and Payne, G. F. (2018) Signal Processing Approach to Probe Chemical Space for Discriminating Redox Signatures. *Biosens. Bioelectron.* 112, 127–135.
- (30) VanArsdale, E., Tsao, C., Liu, Y., Chen, C., Payne, G. F., and Bentley, W. E. (2019) Redox-Based Synthetic Biology Enables Electrochemical Detection of the Herbicides Dicamba and Roundup via Rewired Escherichia Coli. ACS Sensors 4 (5), 1180–1184.
- (31) Daunert, S., Barrett, G., Feliciano, J. S., Shetty, R. S., Shrestha, S., and Smith-Spencer, W. (2000) Genetically Engineered Whole-Cell Sensing Systems: Coupling Biological Recognition with Reporter Genes. *Chem. Rev.* 100 (7), 2705–2738.
- (32) Tschirhart, T., Zhou, X. Y., Ueda, H., Tsao, C.-Y., Kim, E., Payne, G. F., and Bentley, W. E. (2016) Electrochemical Measurement of the β -Galactosidase Reporter from Live Cells: A Comparison to the Miller Assay. *ACS Synth. Biol.* 5 (1), 28–35.
- (33) Su, L., Jia, W., Hou, C., and Lei, Y. (2011) Microbial Biosensors: A Review. *Biosens. Bioelectron.* 26 (5), 1788–1799.
- (34) Sun, J.-Z., Peter Kingori, G., Si, R.-W., Zhai, D.-D., Liao, Z.-H., Sun, D.-Z., Zheng, T., and Yong, Y.-C. (2015) Microbial Fuel Cell-Based Biosensors for Environmental Monitoring: A Review. *Water Sci. Technol.* 71 (6), 801–809.
- (35) Hörnström, D., Larsson, G., van Maris, A. J. A., and Gustavsson, M. (2019) Molecular Optimization of Autotransporter-Based Tyrosinase Surface Display. *Biochim. Biophys. Acta, Biomembr.* 1861 (2), 486–494.
- (36) Gustavsson, M., Hörnström, D., Lundh, S., Belotserkovsky, J., and Larsson, G. (2016) Biocatalysis on the Surface of Escherichia Coli: Melanin Pigmentation of the Cell Exterior. *Sci. Rep.* 6 (1), 36117
- (37) Riley, P. A. (1997) Melanin. Int. J. Biochem. Cell Biol. 29 (11), 1235–1239.
- (38) Mason, H. S. (1948) The Chemistry of Melanin: III. Mechanism of the Oxidation of Dihydroxyphenylalanine by Tyrosinase. *J. Biol. Chem.* 172 (1), 83–99.
- (39) Halaouli, S., Asther, M., Sigoillot, J.-C., Hamdi, M., and Lomascolo, A. (2006) Fungal Tyrosinases: New Prospects in Molecular Characteristics, Bioengineering and Biotechnological Applications. *J. Appl. Microbiol.* 100 (2), 219–232.
- (40) Zaidi, K. U., Ali, A. S., Ali, S. A., and Naaz, I. (2014) Microbial Tyrosinases: Promising Enzymes for Pharmaceutical, Food Bioprocessing, and Environmental Industry. *Biochem. Res. Int.* 2014, 1–16.
- (41) Min, K., Park, K., Park, D.-H., and Yoo, Y. J. (2015) Overview on the Biotechnological Production of L-DOPA. *Appl. Microbiol. Biotechnol.* 99 (2), 575–584.
- (42) Jensen, S. I., Lennen, R. M., Herrgård, M. J., and Nielsen, A. T. (2016) Seven Gene Deletions in Seven Days: Fast Generation of Escherichia Coli Strains Tolerant to Acetate and Osmotic Stress. *Sci. Rep.* 5 (1), 17874.
- (43) Guevara-Martínez, M., Perez-Zabaleta, M., Gustavsson, M., Quillaguamán, J., Larsson, G., and van Maris, A. J. A. (2019) The Role of the Acyl-CoA Thioesterase "YciA" in the Production of (R)-3-Hydroxybutyrate by Recombinant Escherichia Coli. *Appl. Microbiol. Biotechnol.* 103 (9), 3693–3704.
- (44) Datsenko, K. A., and Wanner, B. L. (2000) One-Step Inactivation of Chromosomal Genes in Escherichia Coli K-12 Using PCR Products. *Proc. Natl. Acad. Sci. U. S. A.* 97 (12), 6640–6645.
- (45) Gibson, D. G., Young, L., Chuang, R.-Y., Venter, J. C., Hutchison, C. A., and Smith, H. O. (2009) Enzymatic Assembly of DNA Molecules up to Several Hundred Kilobases. *Nat. Methods* 6 (5), 343–345.
- (46) Dietrich, L. E. P., Price-Whelan, A., Petersen, A., Whiteley, M., and Newman, D. K. (2006) The Phenazine Pyocyanin Is a Terminal Signalling Factor in the Quorum Sensing Network of Pseudomonas Aeruginosa. *Mol. Microbiol.* 61 (5), 1308–1321.

- (47) Webster, T. A., Sismaet, H. J., Conte, J. L., Chan, I. J., and Goluch, E. D. (2014) Electrochemical Detection of Pseudomonas Aeruginosa in Human Fluid Samples via Pyocyanin. *Biosens. Bioelectron.* 60, 265–270.
- (48) Bellin, D. L., Sakhtah, H., Rosenstein, J. K., Levine, P. M., Thimot, J., Emmett, K., Dietrich, L. E. P., and Shepard, K. L. (2014) Integrated Circuit-Based Electrochemical Sensor for Spatially Resolved Detection of Redox-Active Metabolites in Biofilms. *Nat. Commun.* 5 (1), 3256.
- (49) Lindsay, A., and Ahmer, B. M. M. (2005) Effect of SdiA on Biosensors of N-Acylhomoserine Lactones. *J. Bacteriol.* 187 (14), 5054–5058.
- (50) Rivas, G. A., and Solis, V. M. (1991) Indirect Electrochemical Determination of L-Tyrosine Using Mushroom Tyrosinase in Solution. *Anal. Chem.* 63 (23), 2762–2765.
- (51) Rivas, G., and Solis, V. M. (1992) Electrochemical Determination of the Kinetic Parameters of Mushroom Tyrosinase. *Bioelectrochem. Bioenerg.* 29 (1), 19–28.
- (52) Tschirhart, T., Kim, E., McKay, R., Ueda, H., Wu, H.-C., Pottash, A. E., Zargar, A., Negrete, A., Shiloach, J., Payne, G. F., et al. (2017) Electronic Control of Gene Expression and Cell Behaviour in Escherichia Coli through Redox Signalling. *Nat. Commun.* 8 (1), 14030
- (53) Gu, M., and Imlay, J. A. (2011) The SoxRS Response of Escherichia Coli Is Directly Activated by Redox-Cycling Drugs Rather than by Superoxide. *Mol. Microbiol.* 79 (5), 1136–1150.
- (54) Singh, A. K., Shin, J.-H., Lee, K.-L., Imlay, J. A., and Roe, J.-H. (2013) Comparative Study of SoxR Activation by Redox-Active Compounds. *Mol. Microbiol.* 90 (5), 983–996.
- (55) Goldfeder, M., Kanteev, M., Adir, N., and Fishman, A. (2013) Influencing the Monophenolase/Diphenolase Activity Ratio in Tyrosinase. *Biochim. Biophys. Acta, Proteins Proteomics* 1834 (3), 629–633.
- (56) Hassan, H. M., and Fridovich, I. (1978) Superoxide Radical and the Oxygen Enhancement of the Toxicity of Paraquat in Escherichia Coli. *J. Biol. Chem.* 253 (22), 8143–8148.
- (57) Ramsden, C. A., and Riley, P. A. (2014) Tyrosinase: The Four Oxidation States of the Active Site and Their Relevance to Enzymatic Activation, Oxidation and Inactivation. *Bioorg. Med. Chem.* 22 (8), 2388–2395.
- (58) Yang, X., Kirsch, J., Zhang, Y., Fergus, J., and Simonian, A. (2014) Electrode Passivation by Phenolic Compounds: Modeling Analysis. *J. Electrochem. Soc.* 161 (8), E3036–E3041.
- (59) Lau, G. W., Hassett, D. J., Ran, H., and Kong, F. (2004) The Role of Pyocyanin in Pseudomonas Aeruginosa Infection. *Trends Mol. Med.* 10 (12), 599–606.
- (60) Sheplock, R., Recinos, D. A., Mackow, N., Dietrich, L. E. P., and Chander, M. (2013) Species-Specific Residues Calibrate SoxR Sensitivity to Redox-Active Molecules. *Mol. Microbiol.* 87 (2), 368–381
- (61) Juminaga, D., Baidoo, E. E. K. K., Redding-Johanson, A. M., Batth, T. S., Burd, H., Mukhopadhyay, A., Petzold, C. J., and Keasling, J. D. (2012) Modular Engineering of L-Tyrosine Production in Escherichia Coli. *Appl. Environ. Microbiol.* 78 (1), 89–98.
- (62) Chávez-Béjar, M. I., Balderas-Hernandez, V. E., Gutiérrez-Alejandre, A., Martinez, A., Bolívar, F., and Gosset, G. (2013) Metabolic Engineering of Escherichia Coli to Optimize Melanin Synthesis from Glucose. *Microb. Cell Fact.* 12 (1), 108.
- (63) Bonde, M. T., Pedersen, M., Klausen, M. S., Jensen, S. I., Wulff, T., Harrison, S., Nielsen, A. T., Herrgård, M. J., and Sommer, M. O. A. (2016) Predictable Tuning of Protein Expression in Bacteria. *Nat. Methods* 13 (3), 233–236.
- (64) Terrell, J. L., Payne, G. F., and Bentley, W. E. (2016) Networking Biofabricated Systems through Molecular Communication. *Nanomedicine* 11 (12), 1503–1506.
- (65) Virgile, C., Hauk, P., Wu, H., and Bentley, W. E. (2019) Plasmid-encoded Protein Attenuates Escherichia Coli Swimming Velocity and Cell Growth, Not Reprogrammed Regulatory Functions. *Biotechnol. Prog.* 35 (3), No. e2778.

- (66) Meyer, A. J., Segall-Shapiro, T. H., Glassey, E., Zhang, J., and Voigt, C. A. (2019) Escherichia Coli "Marionette" Strains with 12 Highly Optimized Small-Molecule Sensors. *Nat. Chem. Biol.* 15 (2), 196–204.
- (67) Hooshangi, S., and Bentley, W. E. (2008) From Unicellular Properties to Multicellular Behavior: Bacteria Quorum Sensing Circuitry and Applications. *Curr. Opin. Biotechnol.* 19 (6), 550–555.
- (68) Saeidi, N., Wong, C. K., Lo, T., Nguyen, H. X., Ling, H., Leong, S. S. J., Poh, C. L., and Chang, M. W. (2011) Engineering Microbes to Sense and Eradicate Pseudomonas Aeruginosa, a Human Pathogen. *Mol. Syst. Biol.* 7 (1), 521.
- (69) Lu, L., Zhang, L., Zhang, X., Huan, S., Shen, G., and Yu, R. (2010) A Novel Tyrosinase Biosensor Based on Hydroxyapatite—Chitosan Nanocomposite for the Detection of Phenolic Compounds. *Anal. Chim. Acta* 665 (2), 146–151.
- (70) Liu, Y., Kim, E., Lee, M. E., Zhang, B., Elabd, Y. A., Wang, Q., White, I. M., Bentley, W. E., and Payne, G. F. (2014) Enzymatic Writing to Soft Films: Potential to Filter, Store, and Analyze Biologically Relevant Chemical Information. *Adv. Funct. Mater.* 24 (4), 480–491.
- (71) Florescu, M., and David, M. (2017) Tyrosinase-Based Biosensors for Selective Dopamine Detection. Sensors 17 (6), 1314.
- (72) Kong, L., Huang, S., Yue, Z., Peng, B., Li, M., and Zhang, J. (2009) Sensitive Mediator-Free Tyrosinase Biosensor for the Determination of 2,4-Dichlorophenol. *Microchim. Acta* 165 (1–2), 203–209.
- (73) Wu, L., Deng, D., Jin, J., Lu, X., and Chen, J. (2012) Nanographene-Based Tyrosinase Biosensor for Rapid Detection of Bisphenol A. *Biosens. Bioelectron.* 35 (1), 193–199.
- (74) Nakagawa, A., Matsumura, E., Koyanagi, T., Katayama, T., Kawano, N., Yoshimatsu, K., Yamamoto, K., Kumagai, H., Sato, F., and Minami, H. (2016) Total Biosynthesis of Opiates by Stepwise Fermentation Using Engineered Escherichia Coli. *Nat. Commun.* 7 (1), 10390.
- (75) Awan, A. R., Shaw, W. M., and Ellis, T. (2016) Biosynthesis of Therapeutic Natural Products Using Synthetic Biology. *Adv. Drug Delivery Rev.* 105, 96–106.
- (76) Minami, H., Kim, J.-S., Ikezawa, N., Takemura, T., Katayama, T., Kumagai, H., and Sato, F. (2008) Microbial Production of Plant Benzylisoquinoline Alkaloids. *Proc. Natl. Acad. Sci. U. S. A. 105* (21), 7393–7398.
- (77) Mejía-Caballero, A., de Anda, R., Hernández-Chávez, G., Rogg, S., Martinez, A., Bolívar, F., Castaño, V. M., and Gosset, G. (2016) Biosynthesis of Catechol Melanin from Glycerol Employing Metabolically Engineered Escherichia Coli. *Microb. Cell Fact.* 15 (1), 161.
- (78) Li, J., Maniar, D., Qu, X., Liu, H., Tsao, C.-Y., Kim, E., Bentley, W. E., Liu, C., and Payne, G. F. (2019) Coupling Self-Assembly Mechanisms to Fabricate Molecularly and Electrically Responsive Films. *Biomacromolecules* 20 (2), 969–978.
- (79) Suderman, R., Bachman, J. A., Smith, A., Sorger, P. K., and Deeds, E. J. (2017) Fundamental Trade-Offs between Information Flow in Single Cells and Cellular Populations. *Proc. Natl. Acad. Sci. U. S. A.* 114 (22), 5755–5760.
- (80) Stephens, K., Pozo, M., Tsao, C.-Y., Hauk, P., and Bentley, W. E. (2019) Bacterial Co-Culture with Cell Signaling Translator and Growth Controller Modules for Autonomously Regulated Culture Composition. *Nat. Commun.* 10 (1), 4129.
- (81) Weber, W., Luzi, S., Karlsson, M., Sanchez-Bustamante, C. D., Frey, U., Hierlemann, A., and Fussenegger, M. (2008) A Synthetic Mammalian Electro-Genetic Transcription Circuit. *Nucleic Acids Res.* 37 (4), No. e33.